AD-A091 564 DEFENSE MAPPING AGENCY AEROSPACE CENTER ST LOUIS AIR --ETC F/G 17/7
THE GLOBAL POSITIONING SYSTEM VERSUS GRAVITY DISTURBANCE MODELI--ETC(U)
1979 J HOPKINS

UNCLASSIFIED NL

END
DATE FILMED
1-8
DTIC

SECURITY CLASSIFICATION OF THIS PAGE (When Data Entered)

LEVEL II

REPORT DOCUMENTATION PAGE		READ INSTRUCTIONS BEFORE COMPLETING FORM
1. REPORT NUMBER	2. GOVT ACCESSION NO. AD-A091564	3. RECIPIENT'S CATALOG NUMBER
4. TITLE (and Subtitle) The Global Positioning System Versus Gravity Disturbance Modeling in an Inertial Navigation System.		5. TYPE OF REPORT & PERIOD COVERED
		6. PERFORMING ORG. REPORT NUMBER
7. AUTHOR(s) John Hopkins		8. CONTRACT OR GRANT NUMBER(s) 1977
9. PERFORMING ORGANIZATION NAME AND ADDRESS Defense Mapping Agency Aerospace Center/GDGA St. Louis AFS, Missouri 63118		10. PROGRAM ELEMENT, PROJECT, TASK AREA & WORK UNIT NUMBERS
11. CONTROLLING OFFICE NAME AND ADDRESS Defense Mapping Agency Aerospace Center/GDGA St. Louis AFS, Missouri 63118		12. REPORT DATE January 1981
		13. NUMBER OF PAGES 19
14. MONITORING AGENCY NAME & ADDRESS (if different from Controlling Office) 12 22		15. SECURITY CLASS. (of this report) Unclassified
		15a. DECLASSIFICATION/DOWNGRADING SCHEDULE

16. DISTRIBUTION STATEMENT (of this Report)

Distribution is Unlimited

DTIC ELECTE OCT 30 1980 S D E

17. DISTRIBUTION STATEMENT (of the abstract entered in Block 20, if different from Report)

18. SUPPLEMENTARY NOTES

19. KEY WORDS (Continue on reverse side if necessary and identify by block number)

Global Positioning System
Gravity Disturbance Vector
Finite Element Modeling
Inertial Navigation System

3395

20. ABSTRACT (Continue on reverse side if necessary and identify by block number)

The Global Positioning System provides a real-time means of updating an aircraft inertial navigation system to reduce position and velocity errors due, in part, to an inexact knowledge of the gravity field in which the aircraft is flying. Gravity disturbance modeling via such techniques as point mass or finite element modeling provides a real-time means of reducing this gravity field error. This paper demonstrates that should the navigator be denied the GPS signal, the modeling of gravity disturbances can adequately minimize the navigation error.

DD FORM 1 JAN 73 1473 EDITION OF 1 NOV 65 IS OBSOLETE

407789

SECURITY CLASSIFICATION OF THIS PAGE (When Data Entered)

In the presence of the GPS signal, the gravity disturbance component information, combined with GPS data via Kalman filtering, constitutes a further refinement in the system.

3303

THE GLOBAL POSITIONING SYSTEM
VERSUS
GRAVITY DISTURBANCE MODELING
IN AN
INERTIAL NAVIGATION SYSTEM

BY

John Hopkins

Presented to

19th AIAA Aerospace Sciences Meeting
St. Louis, Missouri
January 1981

Defense Mapping Agency
Aerospace Center
St. Louis Air Force Station, Missouri 63118

DASD #3395

THE GLOBAL POSITIONING SYSTEM

VERSUS

GRAVITY DISTURBANCE MODELING

IN AN

INERTIAL NAVIGATION SYSTEM

Abstract

The Global Positioning System provides a real-time means of updating an aircraft inertial navigation system to reduce position and velocity errors due, in part, to an inexact knowledge of the gravity field in which the aircraft is flying. Gravity disturbance modeling via such techniques as point mass or finite element modeling provides a real-time means of reducing this gravity field error. This paper demonstrates that should the navigator be denied the GPS signal, the modeling of gravity disturbances can adequately minimize the navigation error. In the presence of the GPS signal, the gravity disturbance component information, combined with GPS data via Kalman filtering, constitutes a further refinement in the system.

THE GLOBAL POSITIONING SYSTEM VERSUS GRAVITY DISTURBANCE MODELING IN AN INERTIAL NAVIGATION SYSTEM

I INTRODUCTION

Recent developments in inertial instrumentation have substantially improved the performance of inertial navigation systems in both aircraft and shipboard applications. The level of confidence in these inertial systems has risen to the point that the geodetic community has begun to utilize inertial instrumentation to perform surveys of geodetic quality (1). In the geodetic survey mode, data from inertial systems are processed post-mission to determine the components of the gravity disturbance vector. However, in the navigation mode, operating in real-time, these gravity disturbance components must somehow be furnished to the inertial navigation system, in which they have now become a significant error source.

In state-of-the-art inertial navigation systems, electrostatically supported gyros have reduced drift rates to as low as 0.000001°/hr and electrostatic accelerometers have reduced accelerometer bias to as low as 1 μg ($\sim 1 \times 10^{-5}$ m/sec/sec) (2). The accelerometer is a specific force instrument, i.e., it measures the total acceleration due to the vehicle, errors and biases, gravity. Hence, the unknown gravity disturbance components act as time dependent accelerometer biases, which, by Einstein's Principle of Equivalence, cannot be separated by instrumentation operating at the acceleration level.

Although the gravity gradiometer shows great promise for real-time determination of the gravity disturbance components (3), the implementation of such a system remains just beyond our grasp. Thus, we are led to the necessity to provide either a means of modeling the gravity disturbance in real-time or a means of updating the inertial navigation system with position and velocity information in real-time, so that the errors induced by the unmodeled gravity disturbances can be minimized.

Position information derived from electronic systems such as VORTAC, DME, LORAN and velocity information derived from Doppler radar is sufficiently accurate for many applications. To satisfy more stringent requirements, the Global Positioning System (GPS) has been developed. When used with appropriate receivers, it is capable of deriving .03 a moving vehicle's position and velocity to an accuracy of 10-20 meters about $\pm$ 8 meters and $\pm$ .05 meters/second (one sigma) (4).

The availability of the Global Positioning System begs the question of whether it negates the necessity of modeling the gravity disturbance vector, i.e. --Whether there is any need to model the gravity disturbance, since we can cancel its effect by using the GPS. This paper answers that question by using error propagation techniques to show the effect of the GPS data in a typical navigation system, both with and without compensation by gravity disturbance modeling.

In the modern inertial navigation system (Figure 1) the gravity vector $\underline{g}$ computed in a feedback loop contains terms due to the earth's gravitational field and due to the earth's rotation:

$$\underline{g} = \underline{G} - \Omega_{ie}\,\Omega_{ie}\,\underline{r} \tag{1}$$

where

$\underline{g}$ = gravity vector

$\underline{G}$ = gravitation vector

Ω_{ie} = skew symmetric matrix form of earth's inertially referenced angular velocity, ω_{ie} = $\begin{bmatrix} 0 & 0 & 0 \\ 0 & 0 & -\omega_{ie} \\ 0 & \omega_{ie} & 0 \end{bmatrix}$

$\underline{r}$ = geocentric position vector of vehicle

Now, the gravitation vector $\underline{G}$ is itself the sum of a reference gravitation vector $\underline{\gamma}$ and the gravity disturbance vector $\underline{\delta g}$:

$$\underline{G} = \underline{\gamma} + \underline{\delta g} \tag{2}$$

Typically, the inertial navigation system computes the components of $\underline{\gamma}$ in terms of those terms which correspond to the mathematical reference figure used for the earth, an ellipsoid. In terms of spherical harmonics, the componets of $\underline{\gamma}$ are given by:

$$\gamma_u = \frac{GM}{r^2}\left[1 - \frac{3}{2} J_2 \left(\frac{R}{r}\right)^2 (3 \cos^2 L - 1) - \frac{5}{8} J_4 \left(\frac{R}{r}\right)^4 (35 \cos^4 L - 30 \cos^2 L + 3)\right]$$

$$\gamma_e = 0 \tag{3}$$

$$\gamma_n = - \frac{3GM}{r^2} \left(\frac{R}{r}\right)^2 \sin L \cos L \left[J_2 + \frac{5}{6} J_4 \left(\frac{R}{r}\right)^2 (7 \cos^2 L - 3)\right]$$

where

GM = gravitational constant times mass of Earth

L = geocentric latitude of vehicle (approximated by geodetic latitude)

R = equatorial radius of earth

J_2, J_4 = second and fourth degree zonal harmonic coefficients of geopotential

The earth rotation term, $\Omega_{ie} \Omega_{ie} \underline{r}$, is computed along with the reference gravitation vector so that we may consider the gravity vector as

$$\underline{g} = \underline{\gamma}^* + \underline{\delta g} \tag{4}$$

where $\underline{\gamma}^*$ = reference gravity vector.

The components of the reference gravity vector are given by

$$\gamma^*_u = \gamma_u + r\omega^2_{ie} \cos^2 L$$

$$\gamma^*_e = 0 \tag{5}$$

$$\gamma^*_n = \gamma_n - r\omega^2_{ie} \sin L \cos L$$

ω_{ie} = earth rotation rate

The gravity disturbance vector, $\underline{\delta g}$, which can be defined via equation (4) as the difference between the actual gravity vector and the reference gravity vector, has a root mean square (RMS) value over the United States of 17 μg in the gravity anomaly or down component (5). Extremes in excess of 100 μg occur. While the RMS values are representative of the gravity disturbance, their actual values are very position dependent, varying with longitude as well as latitude and height. Further, their correlation distances are rather short, about 20 km for the east and north components; the position dependence an ellipsoid. In terms of spherical harmonics, the componets of $\underline{\gamma}$ are given by:

$$\gamma_u = \frac{GM}{r^2}\left[1 - \frac{3}{2} J_2\left(\frac{R}{r}\right)^2 (3\cos^2 L - 1) - \frac{5}{8} J_4\left(\frac{R}{r}\right)^4 (35\cos^4 L - 30\cos^2 L + 3)\right]$$

$$\gamma_e = 0 \tag{3}$$

$$\gamma_n = -\frac{3GM}{r^2}\left(\frac{R}{r}\right)^2 \sin L \cos L \left[J_2 + \frac{5}{6} J_4 \frac{R}{r}^4 \cdot (7\cos^2 L - 3)\right]$$

where

GM = gravitational constant times mass of Earth

L = geocentric latitude of vehicle (approximated by geodetic latitude)

R = equatorial radius of earth

J_2, J_4 = second and fourth degree zonal harmonic coefficients of geopotential

The earth rotation term, $\Omega_{ie}\,\Omega_{ie}\,\underline{r}$, is computed along with the reference gravitation vector so that we may consider the gravity vector as

$$\underline{g} = \underline{\gamma}^* + \underline{\delta g} \tag{4}$$

where $\underline{\gamma}^*$ = reference gravity vector.

The components of the reference gravity vector are given by

$$\gamma^*_u = \gamma_u + r\omega^2_{ie} \cos^2 L$$

$$\gamma^*_e = 0 \tag{5}$$

$$\gamma^*_n = \gamma_n - r\omega^2_{ie} \sin L \cos L$$

ω_{ie} = earth rotation rate

The gravity disturbance vector, $\underline{\delta g}$, which can be defined via equation (4) as the difference between the actual gravity vector and the reference gravity vector, has a root mean square (RMS) value over the United States of 17 μg in the gravity anomaly or down component (5). Extremes in excess of 100 μg occur. While the RMS values are representative of the gravity disturbance, their actual values are very position dependent, varying with longitude as well as latitude and height. Further, their correlation distances are rather short, about 20 km for the east and north components; the position dependence is seen to be rather strong. Thus, it is advisable to incorporate into the gravity computation feedback loop a computation of the gravity disturbance as a function of position.

A rigorous computation of the gravity disturbance components involves a world-wide integration of gravity anomaly data via the equations (6):

$$\delta g_u = \frac{R}{4\pi}\int_\sigma \Delta g \frac{\partial S(r,\psi)}{\partial r}\, d\sigma$$

$$\delta g_e = \frac{R}{4\pi r \cos L}\int_\sigma \Delta g \frac{\partial S(r,\psi)}{\partial \lambda}\, d\sigma \qquad (6)$$

$$\Delta g_n = \frac{R}{4\pi r}\int_\sigma \Delta g \quad \frac{\partial S(r,\psi)}{\partial L}$$

where

Δg = gravity anomaly for surface element $d\sigma$

$S(r,\psi)$ = the extended Stokes Function

$$S(r,\psi) = \frac{2R}{\rho} + \frac{R}{r} - \frac{3R\rho}{r^2} - \frac{R^2}{r}\cos\psi.$$

$$\left[5 + 3\ell n \frac{r - R\cos\psi + \rho}{2r} \right]$$

$$\rho = (r^2 + R^2 - 2Rr\cos\psi)^{1/2}$$

$$\psi = \cos^{-1}(\sin L \sin L' + \cos L \cos L' \cos(\lambda' - \lambda))$$

L', λ' = coordinates of midpoint of surface element to which Δg and $d\sigma$ refer.

σ = surface area of earth

The computer storage and time needed to calculate $\underline{\delta g}$ from these equations make their real-time use impractical. The alternative to this computation is the development of modeling techniques in which the gravity disturbance vector can be accurately represented by some mathematical function which is adaptable to real-time computation and is conservative of avionics computer resources.

Although several mathematical models may be applicable to the gravity disturbance modeling problem, two techniques have shown particular promise in investigations conducted at the Defense Mapping Agency Aerospace Center. The modeling technique which has withstood the test of time and application is the use of point masses

(7). A relatively recent technique, still under investigation at DMA Aerospace Center, is the Finite Element Method in which Chebyshev polynominals are used to model the gravity disturbances in small volumes (finite elements) (8). See references (9) and (10) for results of DMA Aerospace Center investigation into goodness of fit of the Finite Element modeling and the result of gravity disturbance modeling on a selected test flight track.

In the Point Mass Model, the gravity disturbances are given by (7)

$$\delta g_u = GM \sum_{j=1}^{N} -\left(\frac{m_j}{M}\right) \frac{1}{\rho^2} \frac{\partial \rho}{\partial r}$$

$$\delta g_e = GM \sum_{j=1}^{N} -\left(\frac{m_j}{M}\right) \frac{1}{\rho^2} \frac{\partial \rho}{\partial \lambda} \qquad (7)$$

$$\delta g_n = GM \sum_{j=1}^{N} -\left(\frac{m_j}{M}\right) \frac{1}{\rho^2} \frac{\partial \rho}{\partial L}$$

where

ρ = distance from jth point mass to exterior point

$(^{m}j/M)$ = ratio of jth point mass to Earth's mass

N = number of point masses in set.

In the Finite Element Model, the gravity disturbances are given by (8).

$$\delta g_u = \sum_{n=0}^{N} \sum_{i=o}^{n} \sum_{j=o}^{n-1} C_{u_{ijk}} T_i(x_1) T_j(x_2) T_k(x_3)$$

$$\delta g_e = \sum_{n=o}^{N} \sum_{i=o}^{n} \sum_{j=o}^{n-1} C_{e_{ijk}} T_i(x_1) T_j(x_2) T_k(x_3) \qquad (8)$$

$$\delta g_n = \sum_{n=o}^{N} \sum_{i=o}^{n} \sum_{j=o}^{n-1} C_{n_{ijk}} T_i(x_1) T_j(x_2) T_k(x_3)$$

where

N = highest order of approximating polynomials

$k = n-i-j$

$x_1 = (h-h_{ref})/\Delta h$

$x_2 = (\lambda-\lambda_{ref})/\Delta \lambda$

$x_3 = (L-L_{ref})/\Delta L$

$T_n(x)$ = shifted Chebyshev polynomials

$C_{u_{ijk}}, C_{e_{ijk}}, C_{n_{ijk}}$ = coefficients of the set

$h_{ref}, \lambda_{ref}, L_{ref}$ = coordinates of lower southwestern point of cell

$\Delta h, \Delta \lambda, \Delta L$ = dimensions of the cell

In both the Point Mass or Finite Element techniques, the parameters of the fit, (m_j/M) or $C_{u_{ijk}}, C_{e_{ijk}}, C_{n_{ijk}}$, are determined by least square fit to available geopotential data.

In our previous investigations of the Finite Element Method (9), we selected a 9° x 15° x 9 km region (32°N - 41°N, 108°W - 93°W, 0 - 9 km altitude) in the southwestern part of the continental United States (Figure 2) to perform test computations. It was found that third order polynomials would suffice to model the east and north components of the gravity disturbance vector to an accuracy of $\pm$ 5 μg in 102 elements in this area. Of the remaining elements, 29 were adequately modeled with sixth order polynomials (stippled on Figure 2) while the remaining four required ninth order polynomials (stippled and boxed on Figure 2). Along a simulated flight line which carries an aircraft at Mach 0.5 over a mixture of cells requiring third, sixth and ninth order polynomials, we found that if third, sixth and ninth order polynomials were used as required, the modeling accuracy achieved was $\pm$ 2.4 μg in the east component and $\pm$2.7 μg in the north component. This accuracy will be accepted in this paper as representative of that which can be achieved by either Point Mass or Finite Element modeling.

III. ERROR PROPAGATIONS AND KALMAN FILTERING

A semi-continuous Kalman Filter process is used in which the error state vector is propagated by the equation

$$\dot{\underline{X}} = F(t)\, \underline{X} + \underline{W} + \underline{U} \qquad (9)$$

Where

$\underline{X}$ = error state vector

$F(t)$ = fundamental matrix, essentially $\dfrac{\partial \dot{X}}{\partial \underline{X}}$

$\underline{W}$ = vector of error forcing functions

$\underline{U}$ = vector of correcting functions

Assuming that the vertical channel is damped by a barometric or radar altimeter, the state vector consists of east and north position errors, east and north velocity errors and platform orientation errors about the east, north and down axes.

The error covariance matrix is progagated by the equation

$$\dot{P} = F(t)P + PF^T(t) + Q(t) \qquad (10)$$

where

P = error covariance matrix of system

$Q(t)$ = error covariance of forcing functions minus correcting functions if any

Note that $\underline{W}$ is considered to be white noise with zero mean and covariance $Q(t)$.

A discrete Kalman Filter is introduced to incorporate position and velocity updates, data which will be available at discrete intervals. The error state vector is updated by the equation

$$\underline{X}^{(+)} = \underline{X}^{(-)} - K(\underline{Z} - H\underline{X}^{(-)}) \qquad (11)$$

and the error covariance matrix by the equation

$$P^{(+)} = (I - KH)P^{(-)} \qquad (12)$$

where

$\underline{Z}$ = a measurement matrix

H = a matrix relating the measurement to the state vector

in the sense $\underline{Z} = H\underline{X}$

K = the Kalman gain matrix

The matrix $\underline{Z}$ is assumed zero, since the measurement resets the position and velocity with "zero" error.

The Kalman gain matrix is the keystone of the filtering process in that it provides for relative weighting between the error covariance of the state vector and the error covariance of the measurement. It is given by:

$$K = P^{(-)}H(HP^{(-)}H^T - R)^{-1} \tag{13}$$

where

R = error covariance matrix of measurement.

Note: In equations (11) through (13), the superscript $^{(-)}$ implies "immediately before update", and the superscript $^{(+)}$ implies "immediately after update."

A gyro drift rate of 0.000001°/hour and an accelerometer bias of 1 μg were included. In each error propagation, the vector of error forcing functions, $\underline{W}$, includes not only these effects but also the unmodeled gravity disturbance vector $\underline{\delta g}$, which we have computed for all points on the simulated flight line by application of equations (6) to actual gravity data. The error covariance Q of this forcing function is a diagonal matrix with the gravity disturbance variances set to 64×10^{-10} $(\mathrm{m/sec/sec})^2$ for the unmodeled gravity disturbances and equal to the modeling accuracy stated above for the modeled gravity disturbances (11).

Two propagations were accomplished over the flight line depicted on Figure 2 to establish a baseline reflecting the effect of the gravity disturbances with no updating by GPS data. One propagation was accomplished with the vector of correcting functions, $\underline{U}$, equal to zero, representing the error state vector which would result if the gravity disturbances were left unmodeled. The second propagation was accomplished with $\underline{U}$ set equal to the value determined by the Finite Element method as a function of position. Results of these propagations are given in Table I.

TABLE I

Maximum Error State Vector (no GPS Update)

Component	Unmodeled	Modeled
E	1059.24m	31.78m
N	1450.59m	62.10m
$\dot{E}$	1.218m/sec	0.038m/sec
$\dot{N}$	1.598m/sec	0.069m/sec

Three additional sets of propagations were accomplished in order to assess the impact of the GPS data on the inertial navigation system, with and without the gravity disturbance modeling. In these propagations the measurement covariance matrix R is a diagonal matrix with the pertinent elements set equal to the accuracies cited earlier in this paper for the GPS. A measurement is assumed available at each time increment along the flight line. The inertial navigator may use the position data, the velocity data, or both for updating. Table II gives the results for the case where both are used.

TABLE II

Maximum Error State Vector (Position and Velocity Data)

Component	Unmodeled	Modeled
E	73.97m	8.08m
N	42.43m	8.44m
$\dot{E}$	0.233m/sec	0.017m/sec
$\dot{N}$	0.162m/sec	0.019m/sec

The application of the GPS data has improved the unmodeled case by better than an order of magnitude in position and nearly as well in velocity. However, the improvement is not as great as that afforded by gravity disturbance modeling without the GPS data (see Table I). When the inertial navigator is furnished with both GPS data and gravity disturbance modeling, the results are quite dramatic.

Tables III and IV give the results for the cases where position data only and velocity data only, respectively, are used.

TABLE III

Maximum Error State Vector (Position Data Only)

Component	Unmodeled	Modeled
E	82.32m	8.46m
N	47.90m	8.89m
$\dot{E}$	0.255m/sec	0.017m/sec
$\dot{N}$	0.177m/sec	0.019m/sec

TABLE IV

Maximum Error State Vector (Velocity Data Only)

Component	Unmodeled	Modeled
E	248.28m	21.88m
N	220.92m	20.58m
$\dot{E}$	0.284m/sec	0.028m/sec
$\dot{N}$	0.236m/sec	0.026m/sec

The use of position information alone to update the inertial navigator yields error state vectors nearly the same as those using both position and velocity data. The velocity information does not contribute as significantly to the updating process; however, velocity data provides a substantial improvement in the case where gravity disturbances remain unmodeled.

Figures 3 through 6 graphically portray the variations of the error as a quasi-time-dependent accelerometer bias. On these graphics, which are computer drawn, the fainter lines are the position and velocity errors due to the unmodeled gravity disturbance vector, while the heavier lines are the position and velocity errors after compensation for the gravity disturbances has been applied.

Because the updating occurs in a semi-continuous mode, i.e., at each time increment along the flight line, we do not see glitches or a saw-tooth effect in the graphics. Instead, the graphics approximate sine waves with a frequency equal to the Schuler frequency (period = 84 minutes). Higher frequency variations, especially apparent in the velocity graphic, reflect the effect of the short wavelength components of the gravity field.

IV. CONCLUSIONS

Although the GPS provides the most accurate and effective means of providing updated position and velocity data to an inertial navigation system, the error state vector may grow to greater limits than that tolerable in certain applications. Using optimum gravity disturbance modeling techniques, without further updating by the GPS, the maximum error state vector can be made comparable with that obtainable by the GPS. It is seen then as an alternative should GPS be denied to the inertial navigator. The fullest capabilities of both are realized when the inertial navigator has both gravity disturbance modeling and position and velocity updating from the GPS. If, in the interest of conserving computer resources, it is desirable to use only position data in the updates, there is only a minor degradation in performance of the system. Use of only velocity data in the updates offers an improvement over no modeling at all.

REFERENCES

1. Baussus von Luetzow, H.; "Inertial Geodesy - An Overview"; U.S. Army Engineer Topographic Laboratories, Fort Belvoir, Virginia. (Paper presented to the First International Symposium on Inertial Technology for Surveying and Geodesy). (Undated)

2. Hadfield, M. J.; "Location, Navigation and Surveying Adaptability of High Precision ESG Inertial Navigation Systems in the 1980's"; Proceedings, Position, Location and Navigation Symposium (Plans, 1978), San Diego, California; Institute of Electrical and Electronic Engineers; New York, New York; pp 146-152; 6-9 November 1978.

3. Metzger, E. H.; Rotating Gravity Gradiometer for Correcting Inertial Navigating Systems for Deflection of the Vertical; Report No. 9500-920314; Bell Aerospace Company, Buffalo, New York; January 1974.

4. Milliken, R. J. and C. J. Soller; "Principle of Operation of NAVSTAR and System Characteristics", Navigation, Vol. 25, No. 2, Summer 1978, pp 95-106.

5. Kaula, W. M.; "Determination of the Earth's Gravitational Field"; Reviews of Geophysics, Vol. 1, No. 4, November 1963, pp. 507-551.

6. Heiskanen, W. A. and H. Moritz; Physical Geodesy; W. H. Freeman and Company, San Francisco, California; 1967.

7. Hopkins, J.; "Mathematical Models of Geopotential Gradients", Proceedings of the Symposium on Earth's Gravitational Field and Secular Variations in Position; The School of Surveying, University of New South Wales; Sydney, Australia; pp. 93-105; 26-30 November 1973.

8. Junkins, J. L. and J. T. Saunders; Development of Finite Element Models for the Earth's Gravity Field, Phase II - Fine Structure Disturbance Gravity Representations; Technical Report ETL-0097; U.S. Army Engineer Topographic Laboratories, Fort Belvoir, Virginia; March 1977.

9. Richardson, D. A. and J. Hopkins; "Gravity Disturbance Components Computed at Aircraft Altitude Using the Finite Element Method"; Defense Mapping Agency Aerospace Center, St. Louis Air Force Station, Missouri (Paper presented to the Fall Meeting of the American Geophysical Union; San Francisco, California; 4-8 December 1978).

10. Hopkins, J. and D. A. Richardson; "Effects of Unmodeled Gravity Disturbance Components on Inertial Navigation Systems"; Defense Mapping Agency, Aerospace Center, St. Louis Air Force Station, Missouri. (Paper presented to the 35th Annual Meeting of the Institute of Navigation, St. Louis, Missouri; 18-21 June 1979).

11. Chatfield, A. B.; Initial Estimates of the Gravity Model Contributions to Strategic Missile Errors, ASD-TR-78-30; Aeronautical Systems Division, Wright-Patterson Air Force Base, Ohio; August 1978.

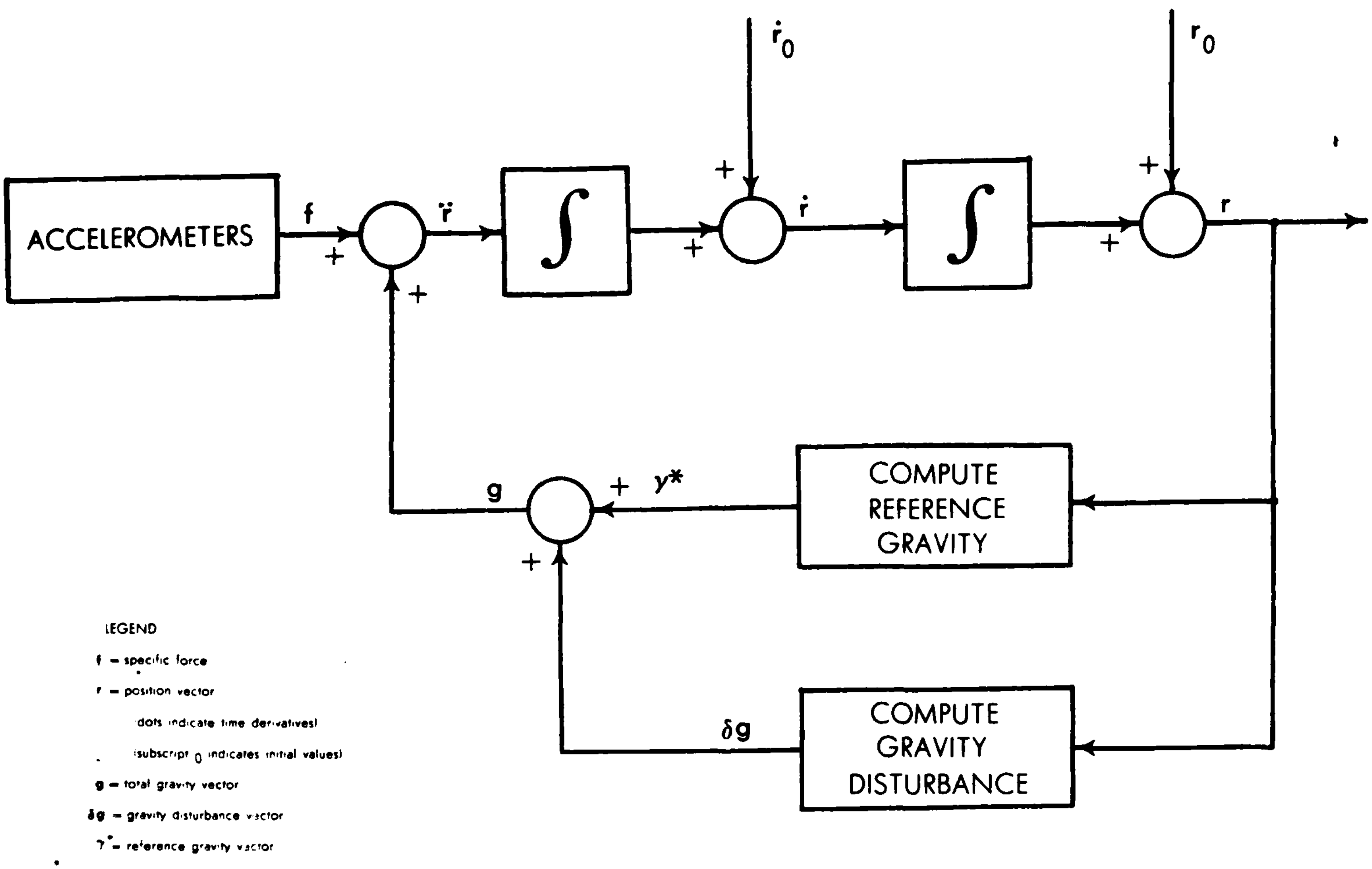

Figure 1. Inertial Navigation System

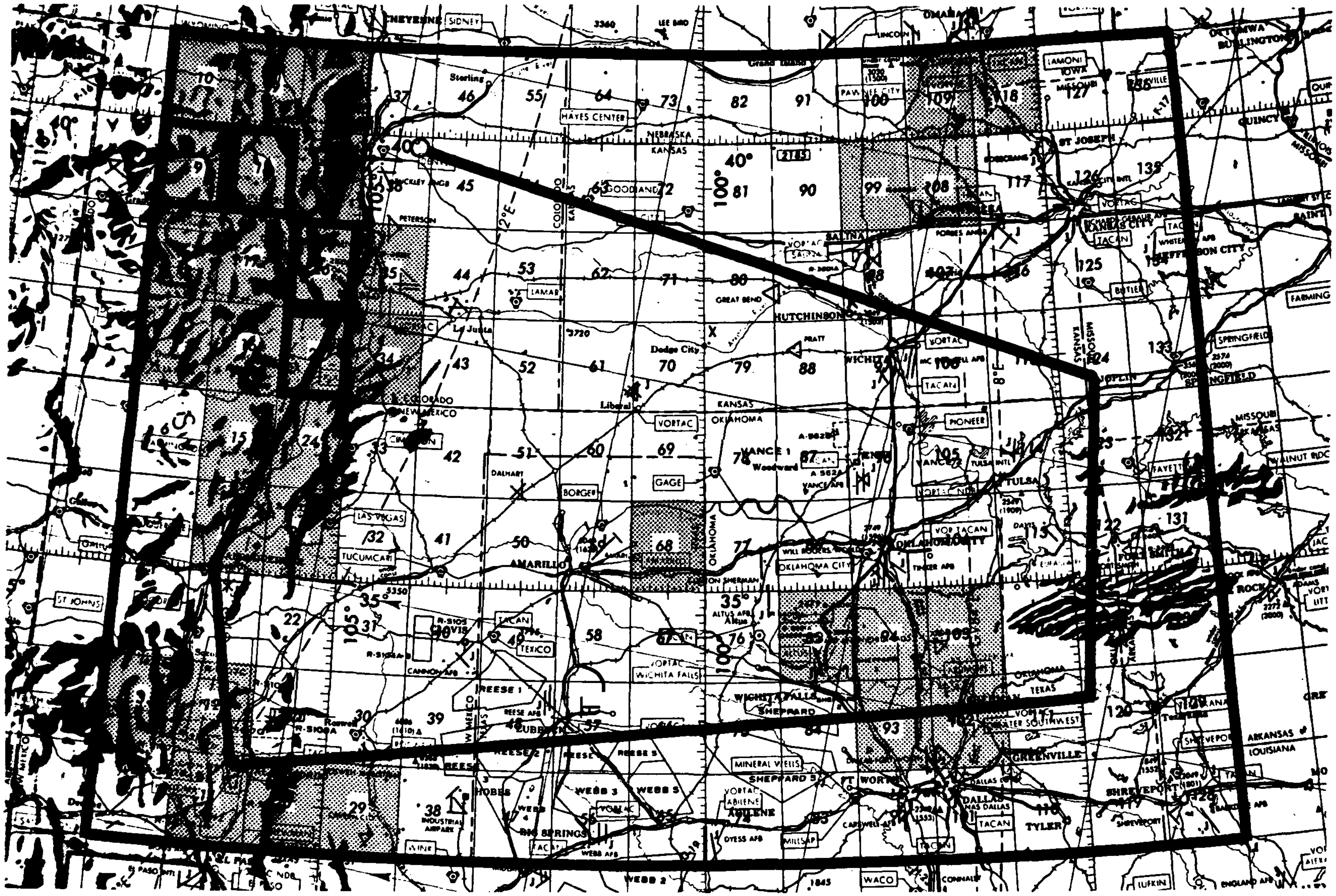

Figure 2. Study Area and Flight Line

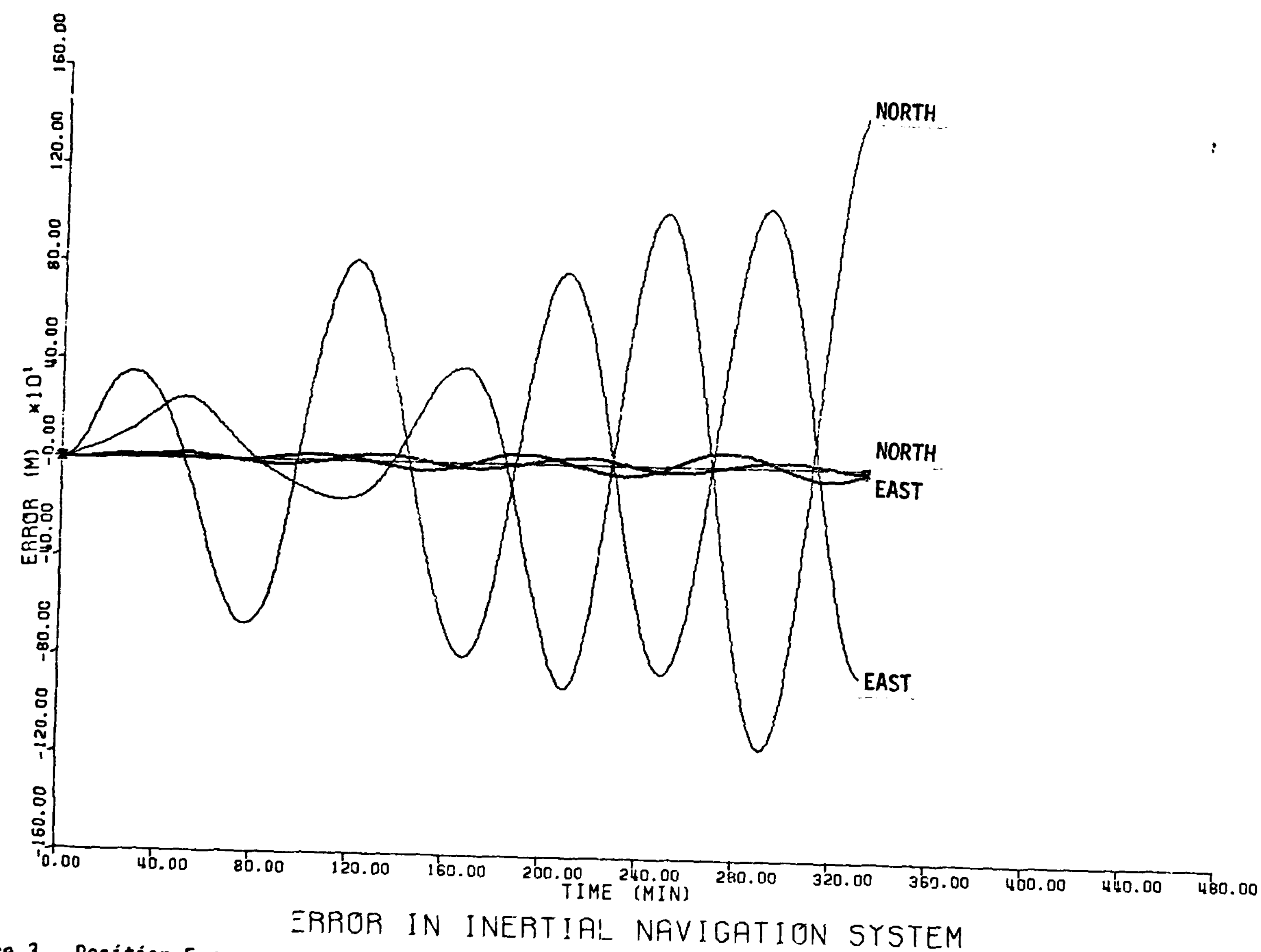

Figure 3. Position Error
No GPS Update

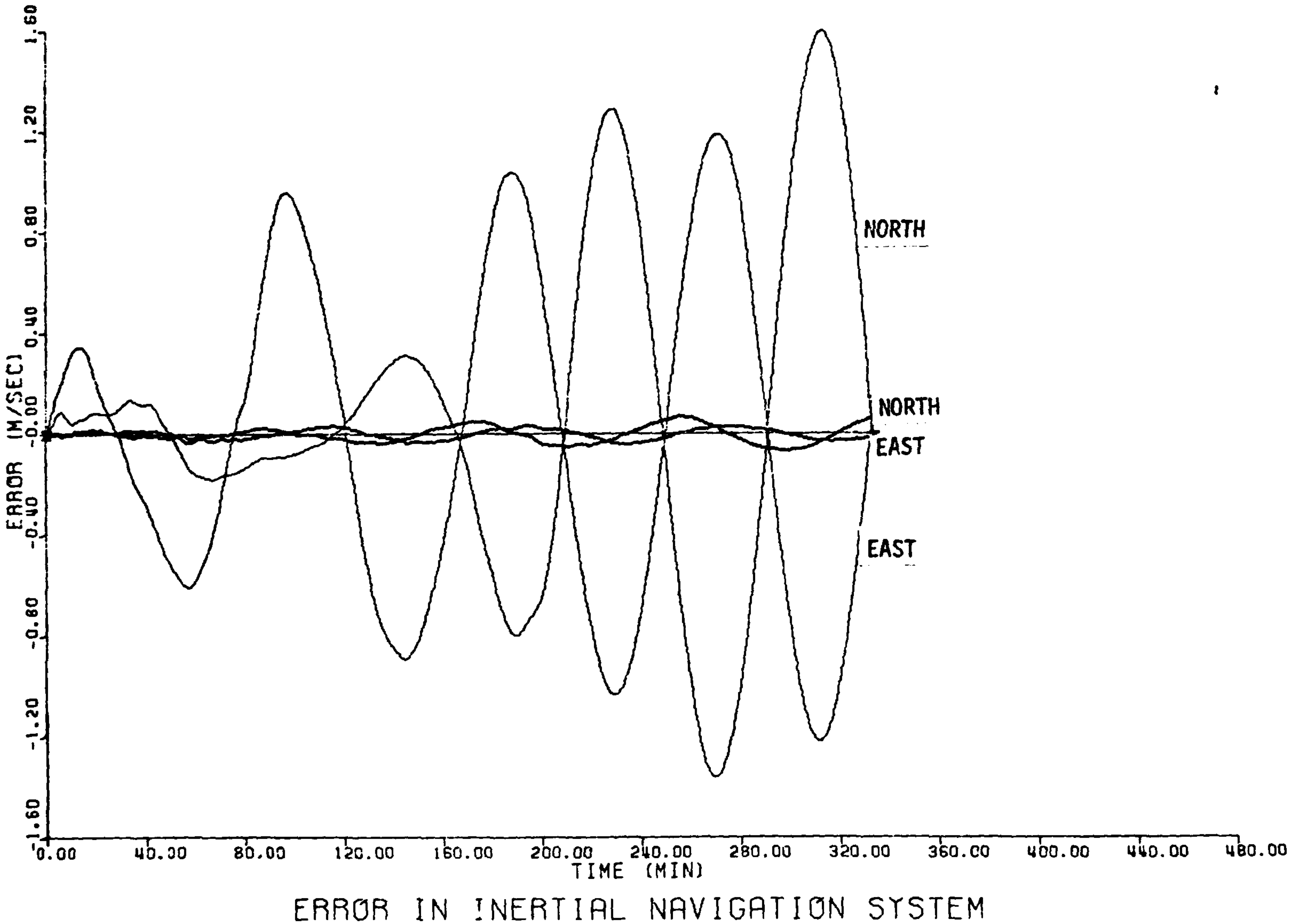

Figure 4. Velocity Error
No GPS Update

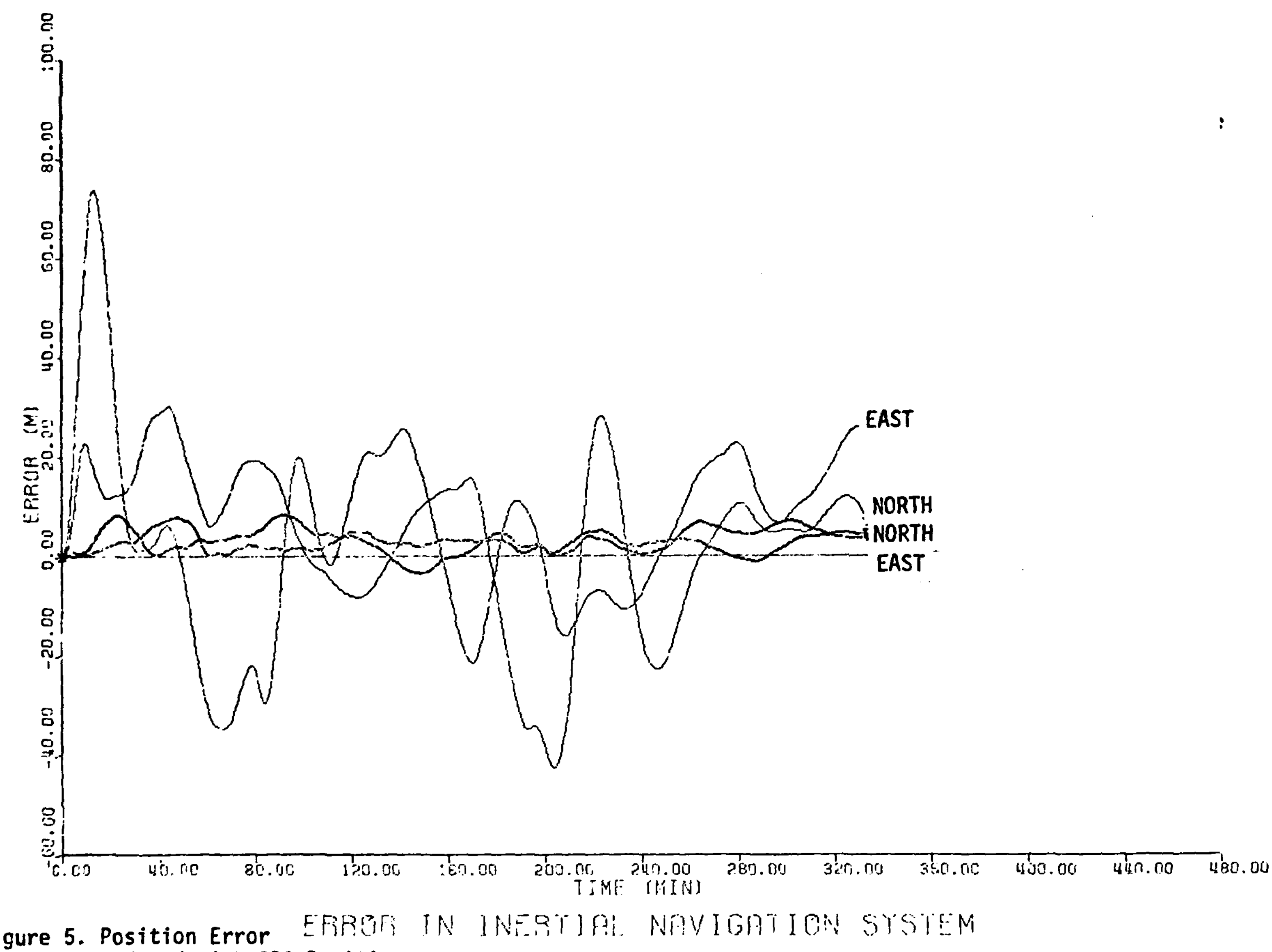

Figure 5. Position Error Updated with GPS Position and Velocity

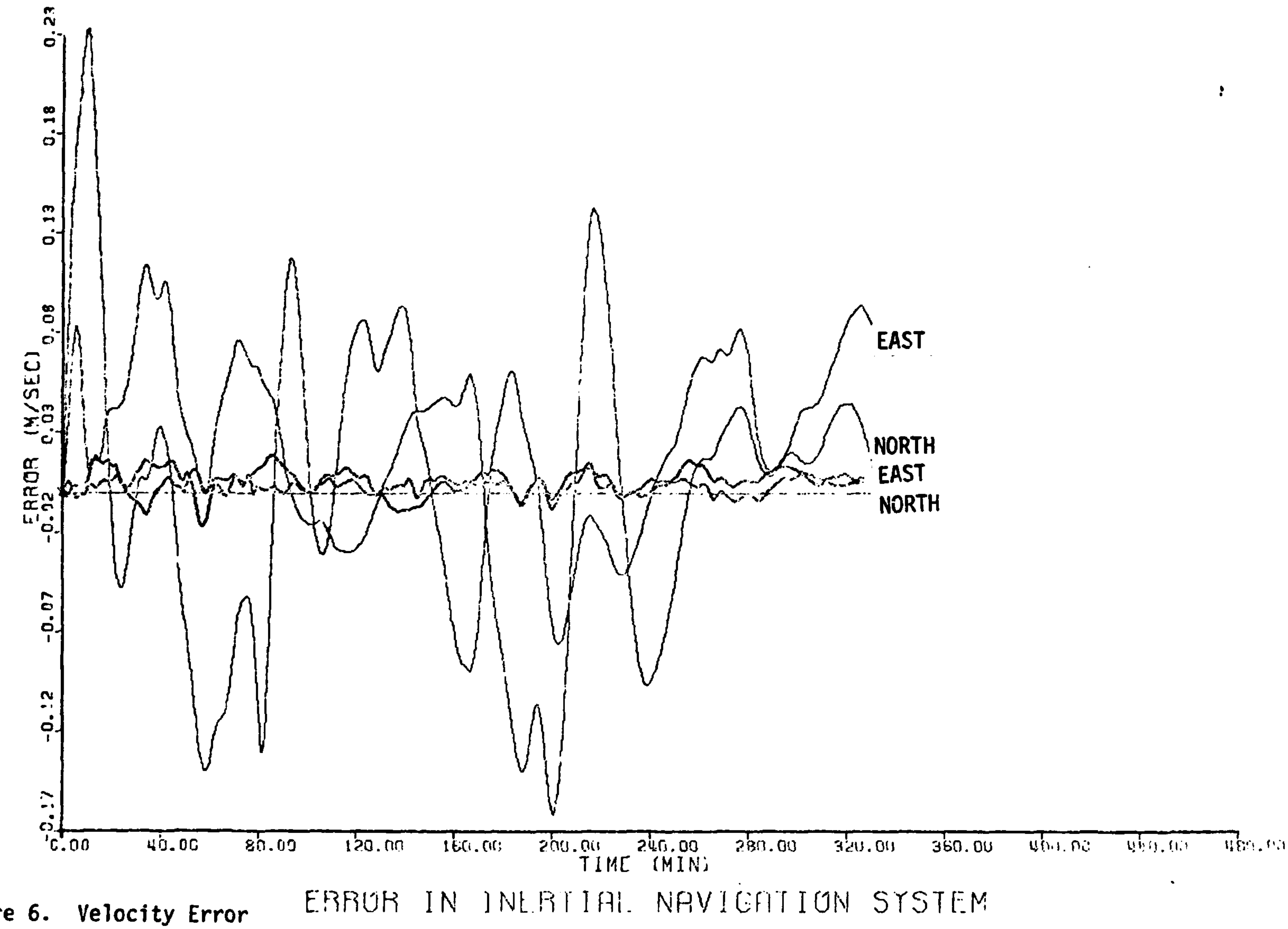

Figure 6. Velocity Error
Updated with GPS Position